Electronic Supplementary Material (ESI) for Nanoscale.

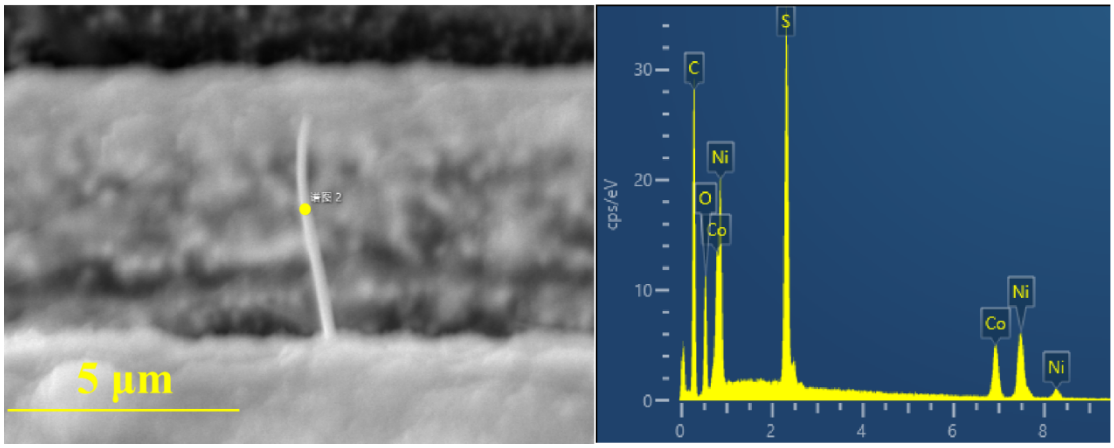

Figure S1. EDS point scanning energy spectrum of CPL PEDOT.

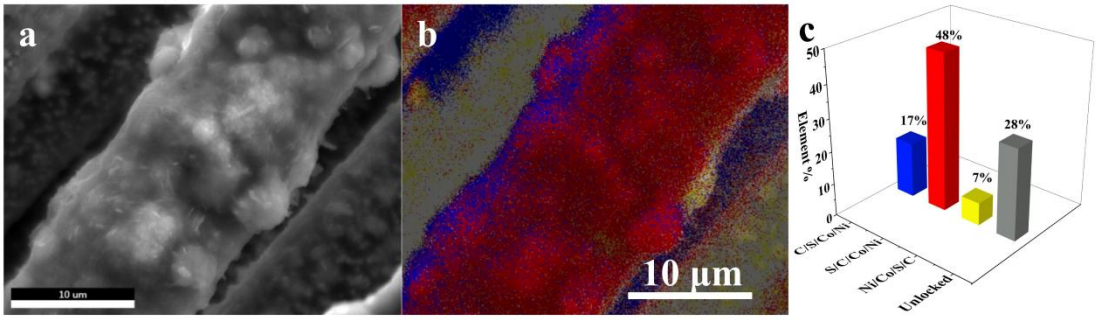

Figure S2. EDAX mapping of Ni-Co(OH)$_2$/CC@PEDOT.

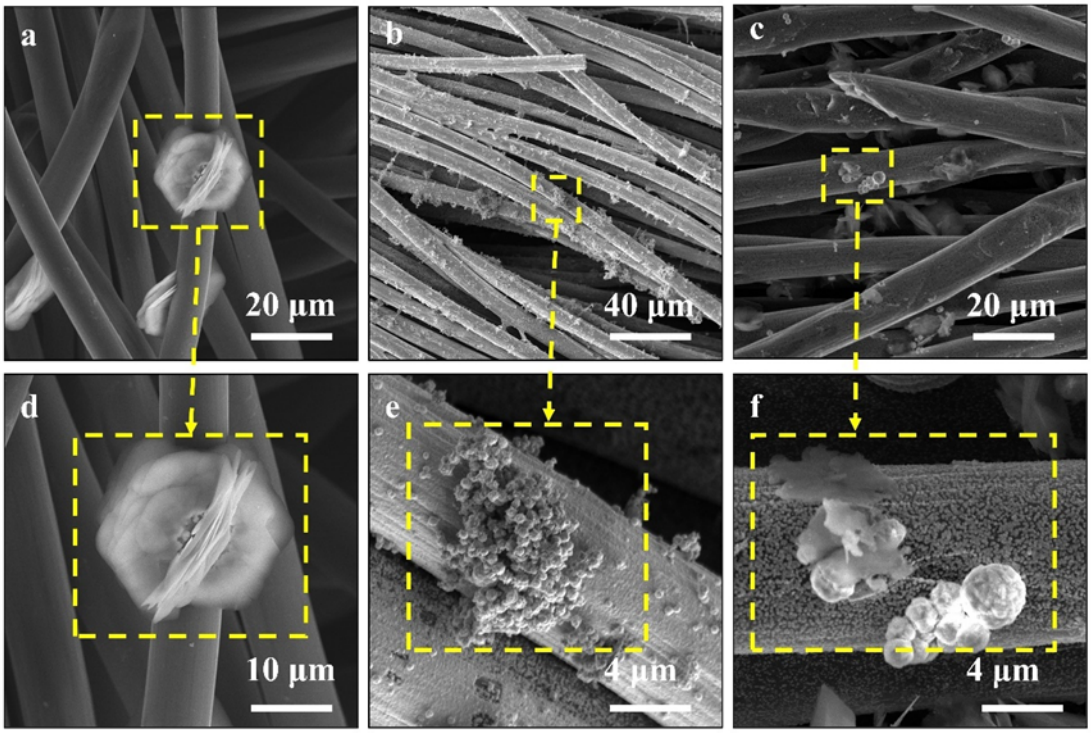

Figure S3. (a-c) FE-SEM images of $Co(OH)_2$/CC, Ni/CC, and Ni-$Co(OH)_2$/CC. (d-f) The images are partial enlargement of Figure S3 a-c.

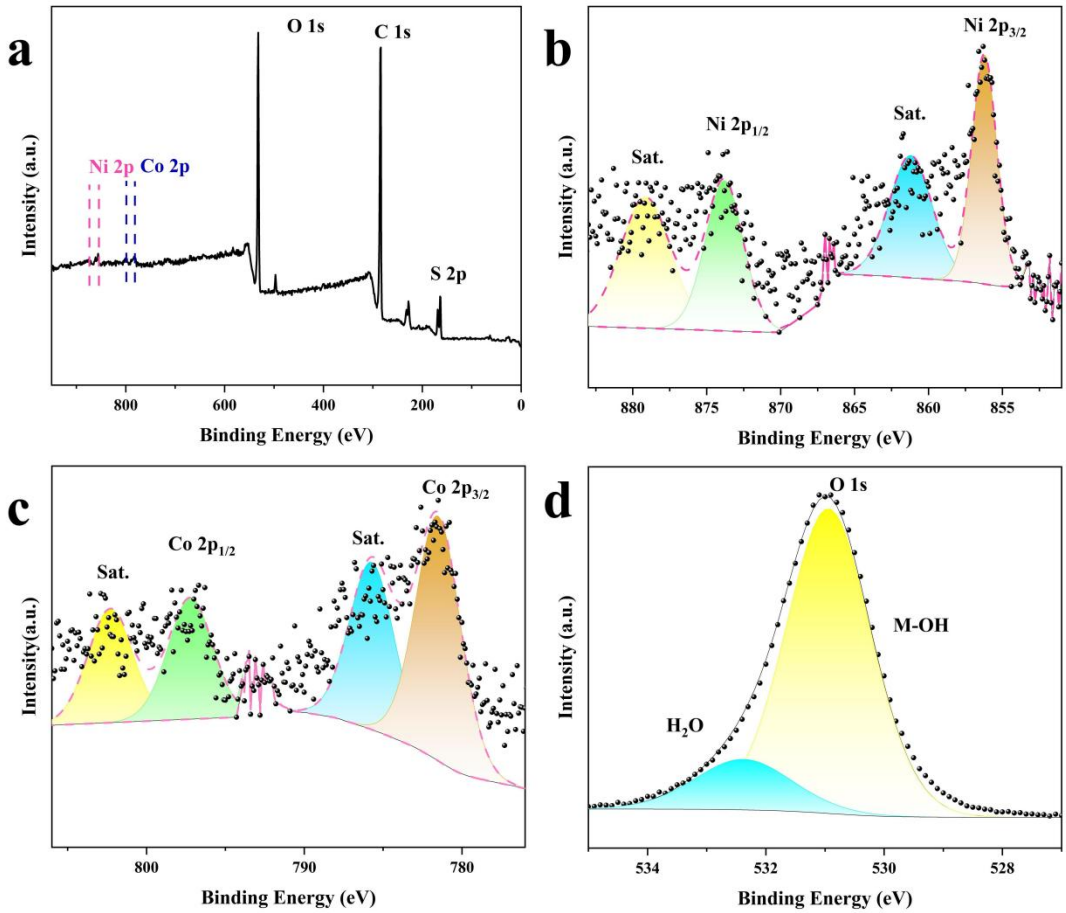

Figure S4. (a) The overall XPS spectrum of the Ni-Co(OH)$_2$/CC@PEDOT composite and high-resolution spectra of (b) Co 2p, (c) Ni 2p, and (d) O 1s.

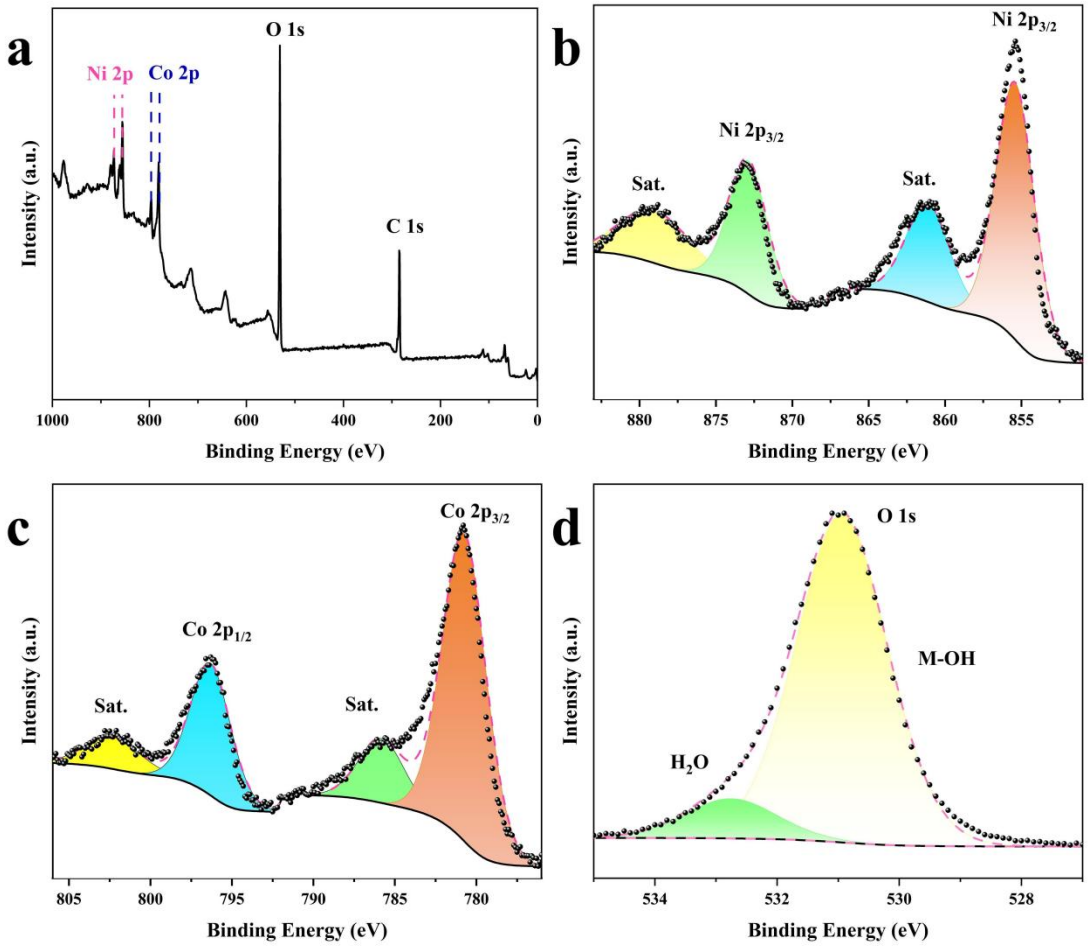

Figure S5. (a) The overall XPS spectrum of the Ni-$Co(OH)_2$/CC composite and high-resolution spectra of (b) Co 2p, (c) Ni 2p, and (d) O 1s.

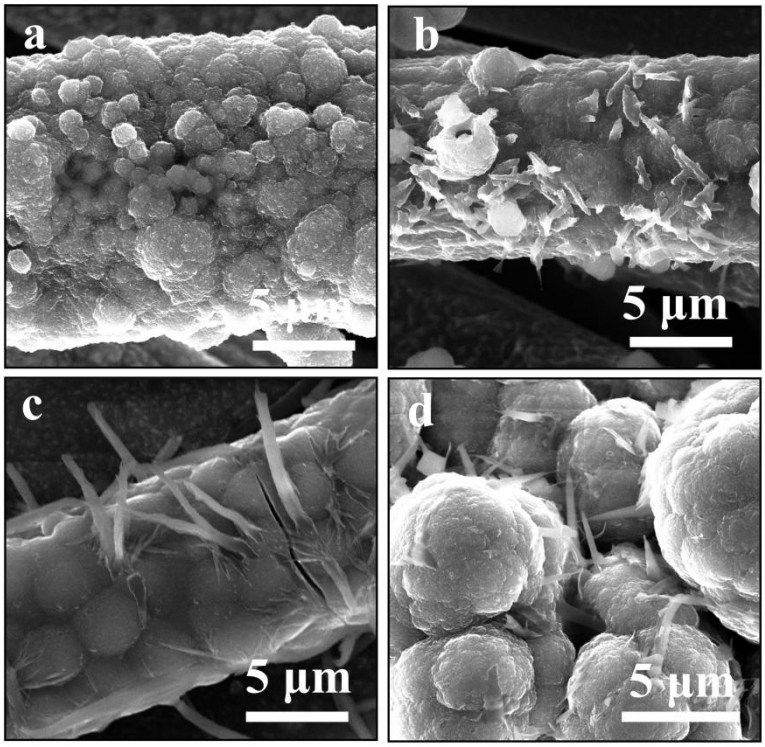

Figure S6. (a-d) SEM images of Ni-Co$(OH)_2$/CC@PEDOT deposited with PEDOT at 1.0 V, 1.1 V, 1.2 V, and 1.3 V.

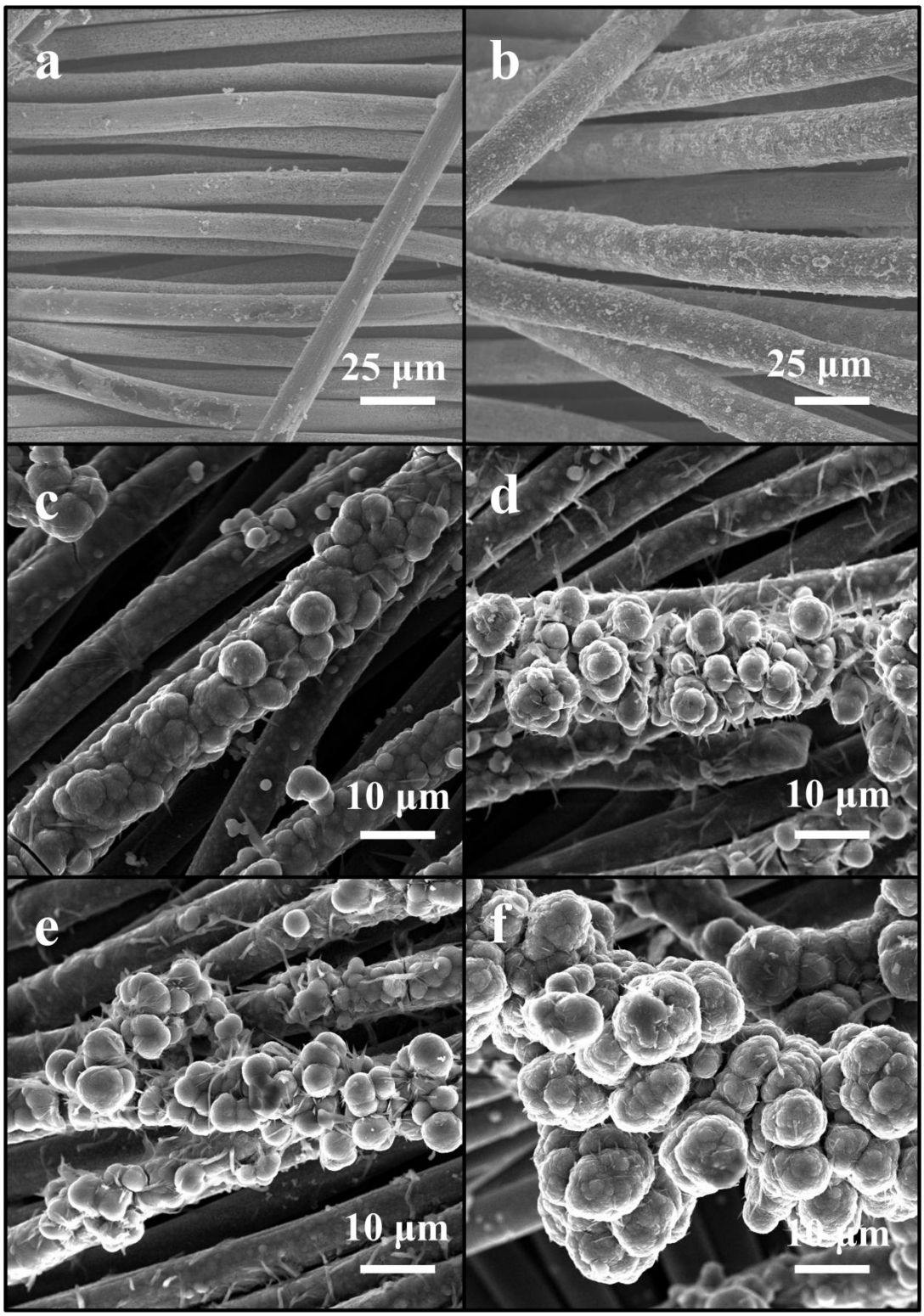

Figure S7. SEM images of Ni-Co$(OH)_2$/CC@PEDOT with deposition potential of 1.2 V and different deposition time (a) 10 s, (b) 20 s, (c) 4 min, (d) 5 min, (e) 6 min, (f) 7 min.

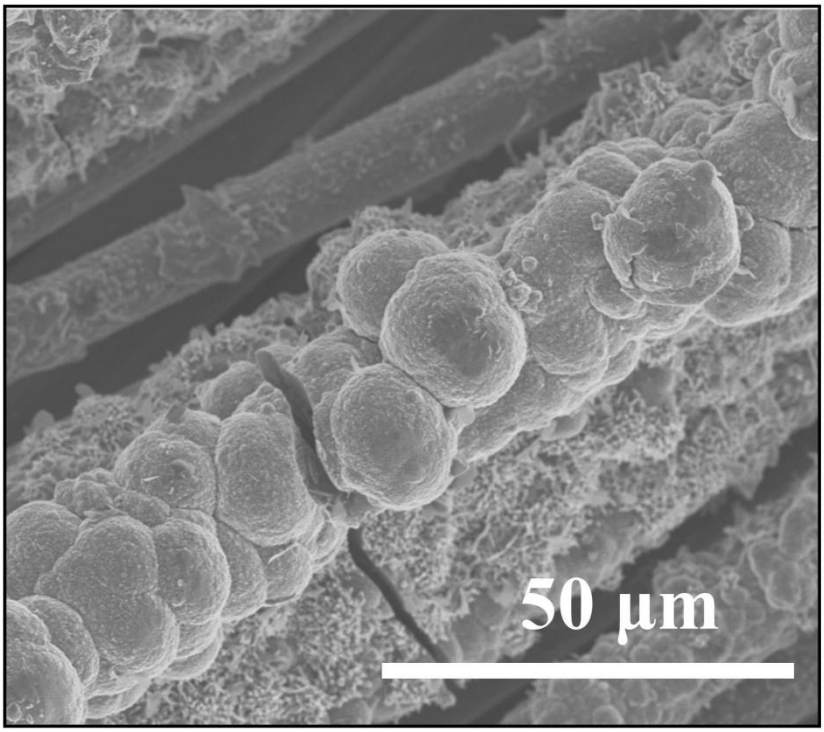

Figure S8. SEM images of Ni-Co$(OH)_2$/CC@PEDOT with deposition potential of 1.2 V and time of 30 min.

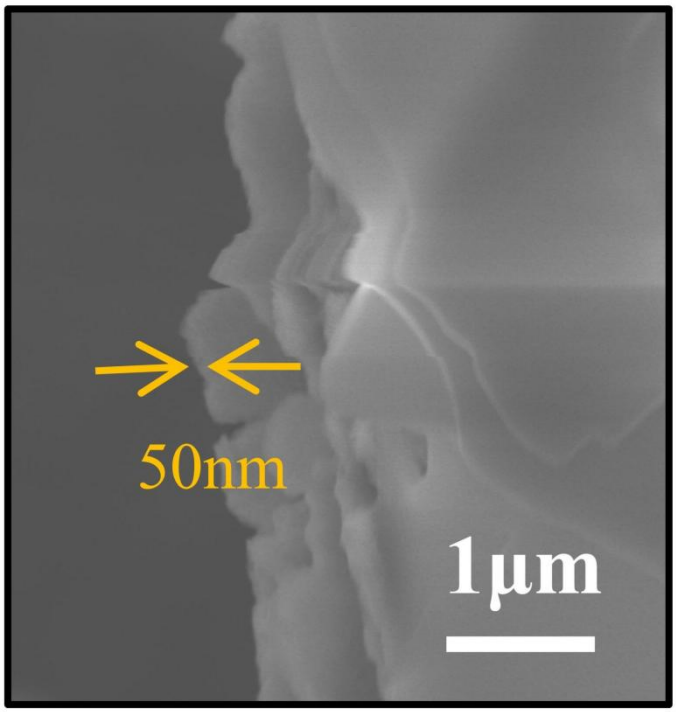

Figure S9. SEM images of cross-section of single CPL PEDOT.

Table S1. The length and average width changes of CPL PEDOT in the bending process.

Time	0 s	5 s	10 s	15 s	20 s	25 s
Average width (μm)	0.08695	0.08956	0.10022	0.11391	0.12583	0.13043
Length (μm)	6.20043	5.83501	5.37782	5.22390	5.10500	4.95717

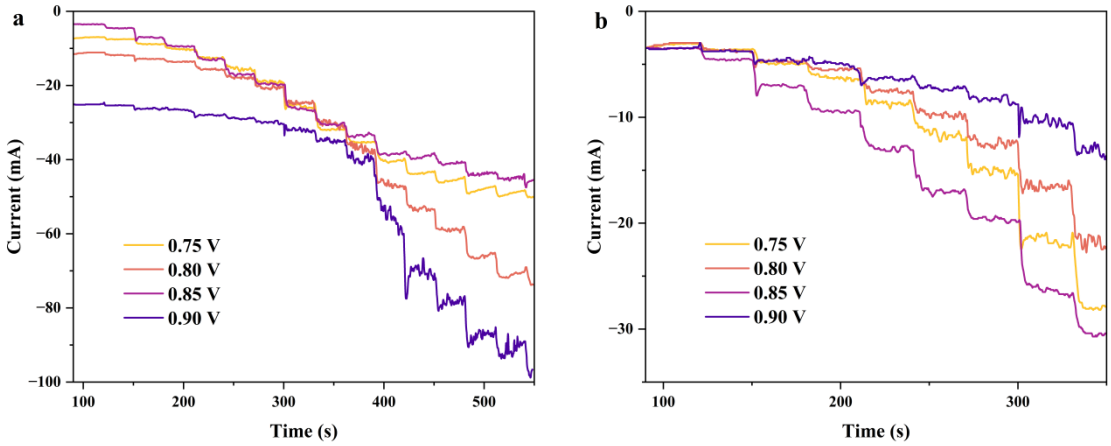

Figure S10. (a) The current response of Ni-Co(OH)$_2$/CC@PEDOT electrodes with different H_2O_2 concentrations at different potentials is continuously decline. (b) Enlarged view of the a-figure section after unification of the initial current platforms.

Table S2. Geometric measurement data for CPL PEDOT.

	Length (nm)	Width (nm)	Height (nm)	Bottom area (nm^2)	Side area (nm^2)	multiplier
1	466	200	6529	93200	4348317	46.65
2	516	180	4388	92880	3054048	32.88
3	526	185	5958	97310	4236138	43.53
4	1154	190	5090	219260	6840960	31.20
5	639	190	4625	121410	3834125	31.58

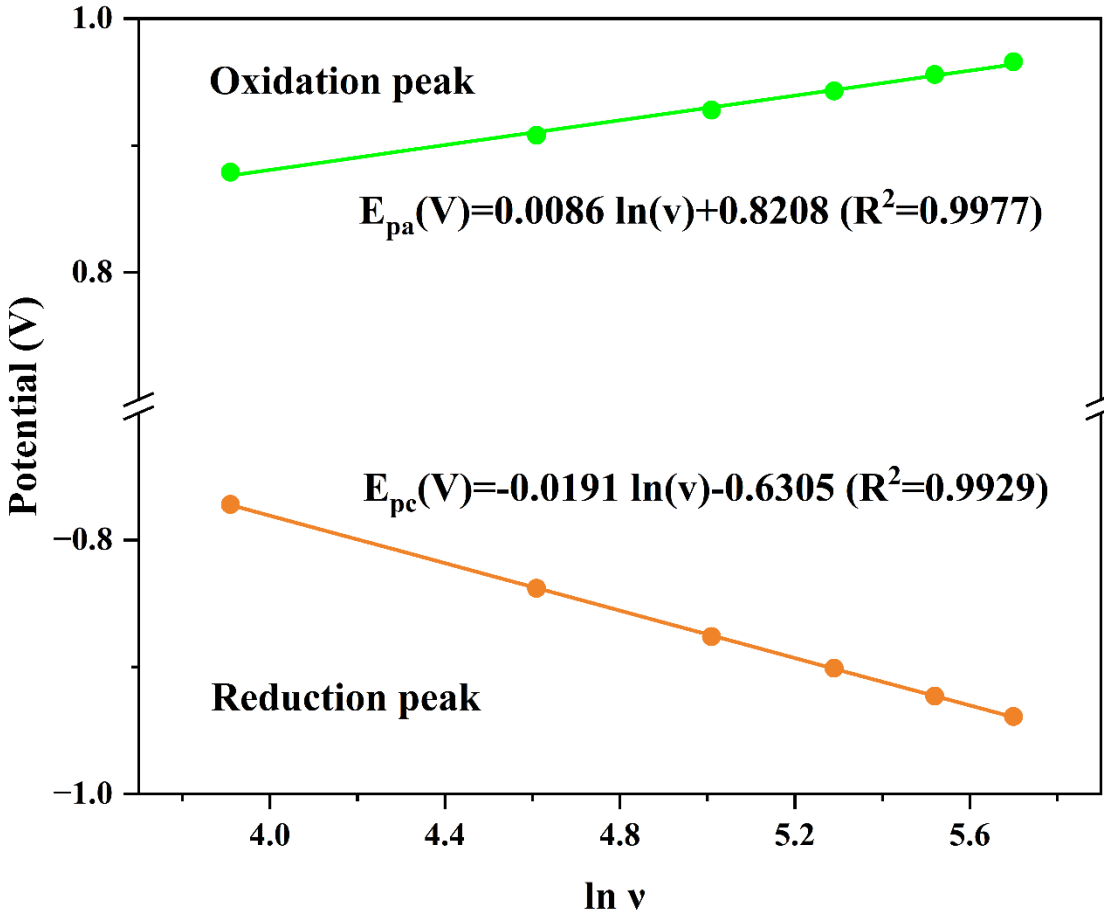

Figure S11. Detection of the change trend of the peak potential with the natural logarithm of the scanning rate at H_2O_2.

Table S3. EIS-related data of CC, Ni-Co$(OH)_2$/CC, and Ni-Co$(OH)_2$/CC@PEDOT electrodes.

Electrodes	R_s（Ω）	R_{ct}（Ω）	W_o-R（Ω）
CC	5.31	2.06	2.16
Ni-Co$(OH)_2$/CC	5.57	1.77	1.49
Ni-Co$(OH)_2$/CC@PEDOT	5.07	1.59	0.35

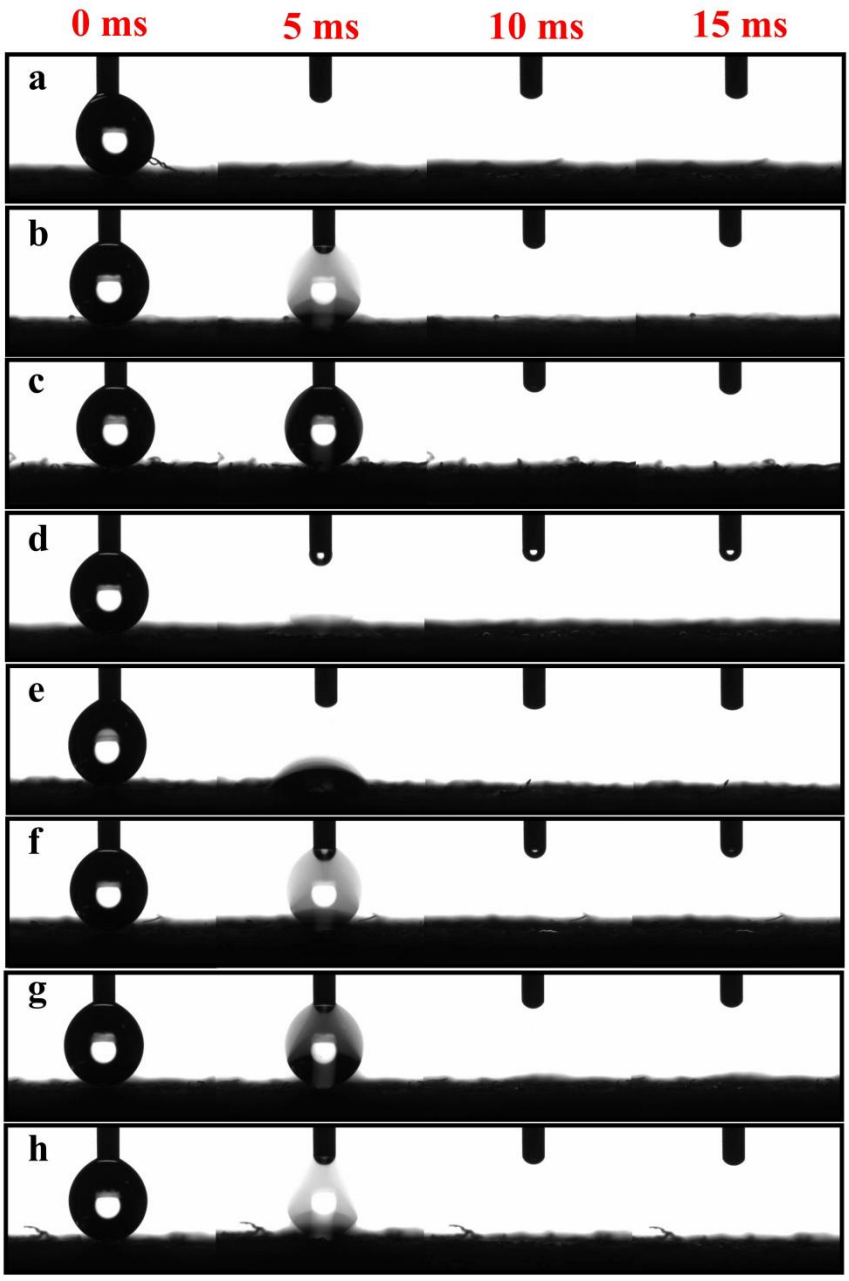

Figure S12. The wetting process of 5 μL water droplets on the surface of Ni-Co(OH)$_2$/CC@PEDOT with different electrochemical deposition parameters. (a) 1.0 V - 5 min, (b) 1.1 V - 5 min, (c) 1.3 V - 5 min, (d) 1.2 V - 3 min, (e) 1.2 V - 4 min, (f) 1.2 V - 5 min, (g) 1.2 V - 6 min, (h) 1.2 V - 7 min.

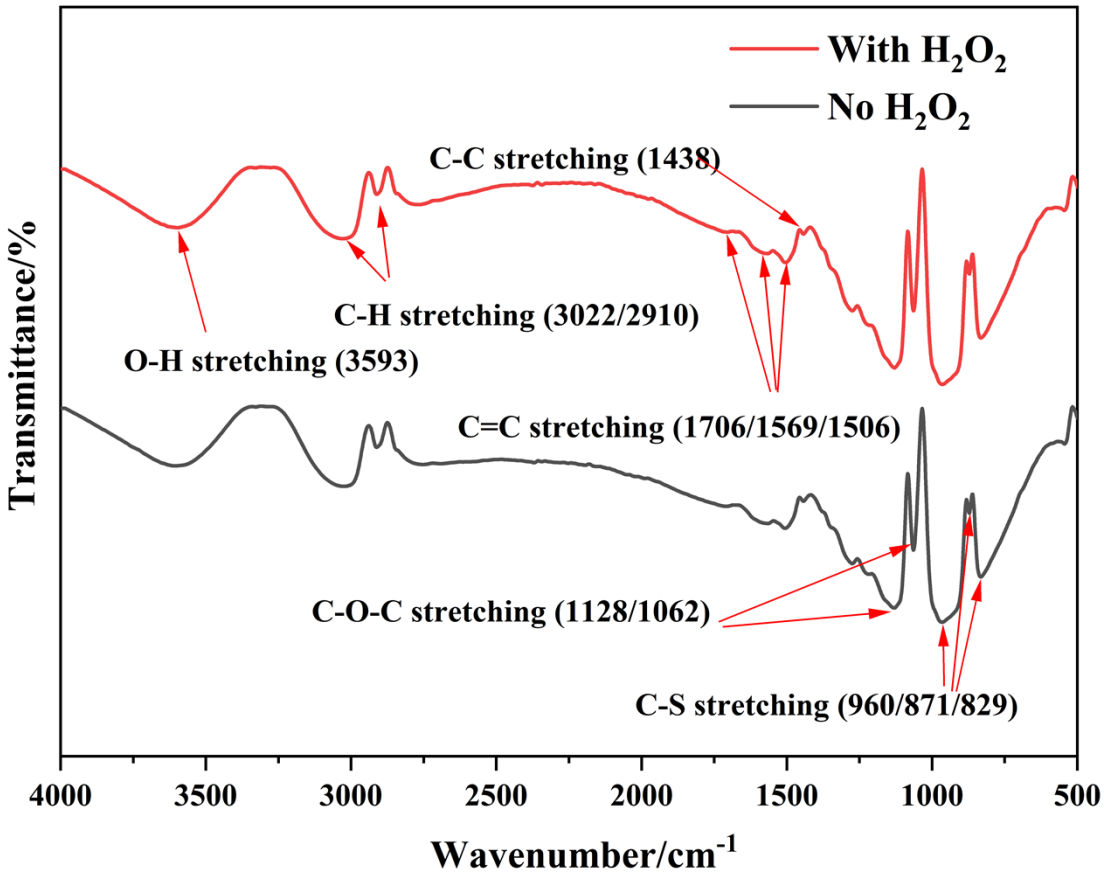

Figure S13. FT-IR spectra of Ni-$Co(OH)_2$/CC@PEDOT (The red curve is obtained after the complexe stay in PBS solution with 3 mM of H_2O_2 for 10 s).

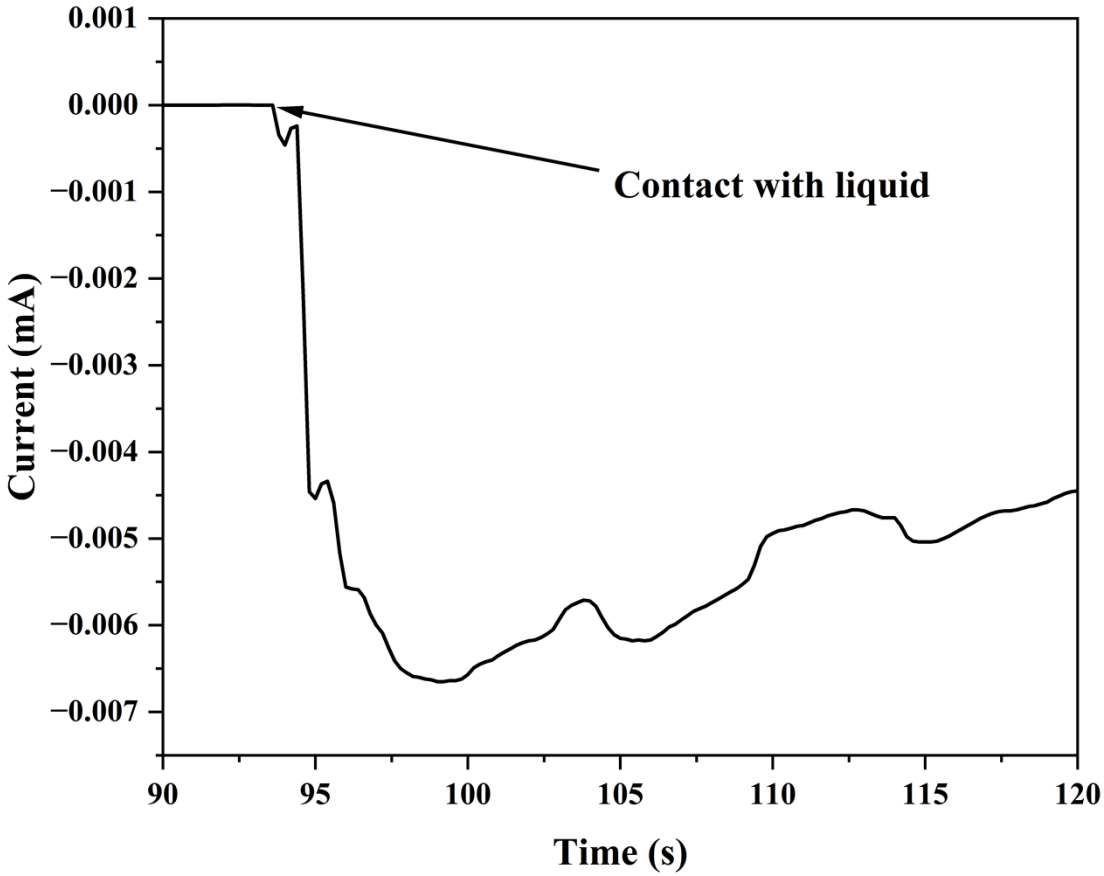

Figure S14. I-t curve of flexible sensors in practical measurement.